



HAL
open science

Determination of the microplastic content in Mediterranean benthic macrofauna by pyrolysis-gas chromatography-tandem mass spectrometry

Magali Albignac, Jean François Ghiglione, Céline Labrune, Alexandra ter
Halle

► **To cite this version:**

Magali Albignac, Jean François Ghiglione, Céline Labrune, Alexandra ter Halle. Determination of the microplastic content in Mediterranean benthic macrofauna by pyrolysis-gas chromatography-tandem mass spectrometry. *Marine Pollution Bulletin*, 2022, 181, pp.113882. 10.1016/j.marpolbul.2022.113882 . hal-03773577

HAL Id: hal-03773577

<https://hal.science/hal-03773577v1>

Submitted on 12 Oct 2023

HAL is a multi-disciplinary open access archive for the deposit and dissemination of scientific research documents, whether they are published or not. The documents may come from teaching and research institutions in France or abroad, or from public or private research centers.

L'archive ouverte pluridisciplinaire **HAL**, est destinée au dépôt et à la diffusion de documents scientifiques de niveau recherche, publiés ou non, émanant des établissements d'enseignement et de recherche français ou étrangers, des laboratoires publics ou privés.

1 Determination of the microplastic content in Mediterranean benthic
2 macrofauna by pyrolysis-gas chromatography-tandem mass
3 spectrometry

4
5 Magali Albignac¹, Jean François Ghiglione², Céline Labrune³, Alexandra ter Halle^{1*}

6
7 ¹CNRS, Université de Toulouse, Laboratoire des Interactions Moléculaires et Réactivité Chimique
8 et Photochimique (IMRCP), UMR 5623, Toulouse, France

9 ²CNRS, Sorbonne Université, Laboratoire d'Océanographie Microbienne (LOMIC), UMR 7621,
10 Observatoire Océanologique de Banyuls, Banyuls sur mer, France

11 ³CNRS, Sorbonne Université, Laboratoire d'Ecogéochimie des Environnements Benthiques
12 (LECOB), UMR 8222, Observatoire Océanologique de Banyuls, Banyuls sur mer, France

13
14 *Corresponding author:

15 Alexandra ter Halle Laboratoire des Interactions Moléculaires et Réactivité Chimique et
16 Photochimique (IMRCP), UMR 5623, 31062 Toulouse Cedex 9, France. Tel.: + 33 (0)561558457.

17 E-mail address: ter-halle@chimie.ups-tlse.fr

18
19
20 **Abstract**

21 The Mediterranean Sea water bodies are ones of the most polluted, especially with
22 microplastics. As the seafloor is the ultimate sink for litter, it is considered a hotspot for
23 microplastic pollution. We provide an original analytical development based on the
24 coupling of tandem mass spectrometry to pyrolysis-gas chromatography to improve the
25 detection of plastic contamination in marine organisms. Due to the high selectivity of the
26 mass spectrometer, a straightforward sample preparation consists uniquely of potassium
27 hydroxide digestion. The quantification of six common polymers is possible in one run.
28 The method was applied to analyze the plastic content from 500 µm down to 0.7 µm in the
29 whole body of seven benthic species with variable feeding modes. Plastic was detected in

30 all samples, with an almost systematic detection of polypropylene and polyethylene. Our
31 method presents a major development in determining the levels of plastic contaminations
32 in samples with rich organic matter content.

33

34 **Keywords**

35 Plastic pollution, marine litter, polymer, bioaccumulation, biodiversity, ingestion, benthic
36 macrofauna

37

38 **Highlights**

39

- 40 • A method for quantifying microplastics in marine organisms down to 0.7 μm was
41 developed using pyrolysis coupled to tandem gas chromatography–mass spectrometry.
- 42 • A one-step sample preparation consisting of chemical digestion was utilized.
- 43 • Six distinct polymer contents were determined in one run.
- 44 • The total polymer contents varied greatly from one organism to the other and was between
45 105 and 7780 $\mu\text{g/g dw}$.
- 46 • The PE, PET and PS polymers were detected the most often.

47

48 **Introduction**

49

50 Plastic loads are increasing in marine ecosystems worldwide (Barnes et al. 2009),
51 and the Mediterranean Sea is one of the most affected marine basins (Consoli et al., 2020;
52 Galgani et al., 1996). Macrolitter densities that exceeded 10^5 items per km^2 were recorded
53 near metropolises (Galgani et al., 2000). Microplastic concentrations (less than 5 mm) on the
54 seafloor, which are considered hotspots of accumulation, can reach up to 1.9 million pieces
55 per m^2 (Kane et al., 2020).

56

57 An initial explanation for microplastic littering is that the litter is transported to the
58 seafloor by vertical settling from surface accumulations and is driven by the density of
59 microplastics. With biofouling, the buoyancy of microplastics is altered, and all types of
60 plastic can sink—whether they are initially buoyant or not (Kooi et al., 2017). Whereas
60 macrolitter sinking may be associated with dense downcanyon flows in the Mediterranean

61 (de Madron et al., 2017; Tubau et al., 2015), microplastic sedimentation in the deep sea is
62 driven more by near-bed thermohaline currents (Kane et al., 2020). In coastal areas,
63 seasonal changes in river flow rate and related turbidity currents also considerably impact
64 the spatial dispersion of litter (Angiolillo et al., 2021).

65 Microplastic hotspots of are also likely hotspots for marine life, as has been shown
66 from the sea surface microlayer (Ghiglione and Laudet, 2020) to deep-sea sediment (Hall,
67 2002; Kane et al., 2020). Marine biota interact with microplastics in several ways, and this
68 leads to a reduction in feeding and depletion in energy stores but also causes toxicity,
69 carcinogenesis, endocrine disruption and physical harm with knock-on effects for fecundity
70 and growth (Galloway et al., 2017). After sedimentation, microplastics are available for
71 many benthic species to feed on, such as detritivores and filter-feeding species (Valente et
72 al., 2020). This potentially impacts the biodiversity throughout marine life, as the benthic
73 community plays an important role in providing resources and ecosystem services
74 (Danovaro et al., 2020; Manea et al., 2020). The extent of the impacts of plastic pollution
75 on Mediterranean ecosystems is poorly estimated, whereas the Mediterranean Sea is a
76 biodiversity hotspot with high levels of endemism (Coll et al., 2010). Monitoring litter-
77 benthic community interactions is largely hampered by difficulties in sampling and the
78 necessary costs (Angiolillo et al., 2021; Valente et al., 2020), which is why the interactions
79 are poorly described even if all reported studies declare that a quasi-systematic of plastic
80 occurs in individuals (Anastasopoulou et al., 2013).

81 In general, microplastics that are larger than 500 μm are visually detected and
82 identified by Fourier Transform Infrared Spectroscopy (FT-IR). There are very few
83 publications that compare microplastics that are smaller than 150 μm . The latest
84 spectroscopic developments allow limits of tens of microns to be reached (Schwaferts et
85 al., 2019), but the detection of the particles is strongly impacted by residual organic matter.
86 This is solved by intensive sample preparations, which are time-consuming and costly
87 forms of analysis that involve risks including altering and losing some microplastics and
88 increasing cross contamination. In this context, pyrolysis-gas chromatography–mass
89 spectrometry (Py-GC–MS) appears to be a very promising technique, even if its
90 developments are very recent (Yakovenko et al., 2020). The use of Py-GC–MS does not
91 have size limitations, and the selectivity of the mass spectrometry offers the possibility to
92 simplify the sample preparation. The use of Py-GC–MS is promising in terms of reducing
93 the time of analysis because several polymers are detected in one run.

94 In addition to all these promising aspects, there are some consequent obstacles with
95 the use of Py-GC-MS (Pico and Barcelo, 2020; (Yakovenko et al., 2020). Two recent
96 studies with important developments resulted, for the first time, in achieving the following
97 robust methods: one for the analysis of biosolids (Okoffo et al., 2020) and the other for
98 seafood samples (Ribeiro et al., 2020). Even if a less intensified purification of the sample
99 is obtained through the use of Py-GC-MS, this step is still important. Okoffo et al. (2020)
100 opted for pressurized liquid extraction, and the remaining organic matter was eliminated
101 during Py-GC-MS analysis using a two-step pyrolysis program (organic matter removal at
102 300 °C followed by pyrolysis at 650 °C). Ribeiro et al. (2020) proposed a more intensified
103 sample purification that involved alkaline digestion followed by pressurized liquid
104 extraction, and they skipped the decomposition step at 300 °C. Here, we introduce the use
105 of tandem mass spectrometry (Py-GC-MS/MS) to enhance the detection performance, thus
106 permitting a simpler sample preparation using alkaline digestion alone. This study aimed
107 to demonstrate that Py-GC-MS/MS is a fast and reliable tool for microplastic
108 quantification down to 0.7 µm in marine organisms. Here, we provide the first assessment
109 of microplastic content in Mediterranean benthic organisms for a selection of 6 different
110 polymers.

111

112 **2. Materials and Methods**

113 **2.1. Chemicals and Reference Materials.**

114 A total of six polymers were targeted. They were chosen among the most abundant
115 polymers in the marine environment, namely, high density polyethylene (PE), poly(methyl
116 methacrylate) (PMMA), polyethylene terephthalate (PET), polycarbonate (PC),
117 polystyrene (PS), and polypropylene (PP). The first three polymers were purchased from
118 Sigma-Aldrich (St. Louis, MO, USA) and the three others were from Goodfellow Group
119 (Huntingdon, United Kingdom). These polymer standards were used to optimize the mass
120 spectrometry conditions and to prepare standards for external calibration. The external
121 calibration was performed with a mix of polymers diluted in a calcined powdered glass
122 microfiber filter (GF/D diameter 47 mm; Whatman® Sigma-Aldrich, St. Louis, MO,
123 USA).

124

125

126 **2.2. Sample Collection and Processing.**

127 All glassware was calcined at 550 °C for 2 hours before use in an incinerator oven
128 (Nabertherm™ LV052K1RN1). Glass fiber filters were calcined at 600 °C for 2 hours
129 before use. Benthic organisms were sampled on the northwestern Mediterranean seafloor
130 from the R/V Nereis II. Specimens sampled with a van veen grab were sorted and stored
131 in a clean metallic bowl on board. At the laboratory, the specimen were identified and
132 placed in calcined glass vials that were closed with a cap, which was equipped with a
133 polytetrafluoroethylene (PTFE) opercula. The details of the GPS location and sampling
134 depth of each organism are given in Table 1. A sampling control consisted of opening a
135 calcined glass vial that contained calcined quartz fiber for approximately the same period
136 of time it took to manipulate the animals both onboard and at the laboratory. The quartz
137 fiber was analyzed by Py-GC–MS/MS similar to the samples. In the laboratory, all animals
138 were freeze-dried and weighed. Under the hood, the animals were transferred to 30 mL
139 glass flasks equipped with glass caps. A ratio of 80 mL per gram of dry animal of 10%
140 potassium hydroxide aqueous solution prefiltered was added. The solution was previously
141 filtered in a closed glass unit from Vagner Glasses Company (Toulouse) on a calcined 47
142 mm diameter membrane with a porosity of 0.45 µm (PTFE Omnipore™, from Sigma–
143 Aldrich, St. Louis, MO, USA) to remove any potential plastic contamination. For the
144 chemical digestion, the flasks were placed in a shaker incubator (Eppendorf®
145 ThermoMixer® C, Sigma–Aldrich, St. Louis, MO, USA) for 48 h at 40 °C with continuous
146 agitation (500 rpm). A similar flask with potassium hydroxide solution and no sample was
147 used as a procedural blank. Once the digestion was completed, the samples were removed
148 from the incubator and prefiltered on 500 µm stainless steel filter grids (Negofiltre, Moret
149 Loing Et Orvanne, France). The solution was then filtered under vacuum with a closed
150 glass unit onto a calcined glass microfiber filter, GF/F diameter 47 mm or 21 mm
151 Whatman® (Sigma–Aldrich, St. Louis, MO, USA). Filters were stored in glass Petri dishes
152 before cryogrinding using the SPEX® SamplePrep 6775 Freezer/Mill cryogenic Grinder
153 (Delta Labo, Avignon) with the program: precool 2 min ; run 1min ; cool 2 min ; cycles
154 15 ; cps 15. A sub-sample of 2 mg was precisely weighted in a microscale with a 10-5 g
155 precision (Micro Balance from Sartorius, MCE225P-2S00-A Cubis®-II Semi) on quartz
156 tubes that were freshly calcined at 1000°C with the pyrolysis probe using the “clean”
157 program. A sub-sample of 2 mg was precisely weighted in a microscale with a 10-5 g
158 precision (Micro Balance from Sartorius, MCE225P-2S00-A Cubis®-II Semi) on quartz

159 tubes that were freshly calcined at 1000°C with the pyrolysis probe using the “clean”
 160 program.

161 **Table 1. List of the benthic organisms that were sampled in the northwestern**
 162 **Mediterranean and analyzed for microplastic contents. The corresponding feeding**
 163 **modes, sampling depths and coordinates are also given.**

164

Taxa	Phylum	Feeding modes	Depth (m)	Coordinate s (WGS84)
<i>Glandiceps talaboti</i>	Enteropneusta	Surface and/or Subsurface deposit feeder	43	42°30.50'N 3°09.11'E
<i>Amphiura chiajei</i>	Echinodermata	Surface deposit feeder	43	42°30.50'N 3°09.11'E
<i>Amphiura filiformis</i>	Echinodermata	Surface deposit and/or suspension feeder	43	42°30.50'N 3°09.11'E
<i>Notomastus sp.</i>	Annelida	Subsurface deposit feeder	43	42°30.50'N 3°09.11'E
<i>Fustiaria rubescens</i>	Molluska	Carnivorous	80	42°30.00'N 3°11.40'E
<i>Acanthocardia sp.</i>	Molluska	Suspension feeder	80	42°30.00'N 3°11.40'E
<i>Lanice conchilega</i>	Annelida	Surface deposit feeder and/or suspension feeder	90	42°30.00'N 3°12.60'E

165

166

167 **2.3 Py-GC–MS/MS Analysis.**

168 The method parameters for analysis by pyrolysis were achieved using a CDS Pyroprobe®
 169 6150 from Quad service (Acheres, France) interfaced with a GC–MS/MS triple quadrupole
 170 TSQ® 9000, GC Trace 1310 from Thermo Fisher Scientific (Villebon sur Yvette, France).
 171 The gas chromatography column was a TraceGOLD TG-5SilMS from Thermo Fisher
 172 Scientific. Samples were pyrolyzed at 600 °C for 30 s. The pyrolysis products were
 173 transferred at 300 °C at the interface and were injected at 300 °C with a split ratio of 15:1
 174 (additional data Table SI 1). Multiple reaction monitoring (MRM) optimizations for

175 collision energy were obtained using Auto SRM 4.0 for Chromeleon software in liquid
176 injection with a Thermo Scientific™ AI/AS 1310 autosampler. The MS
177 acquisition/detection parameters are listed in Table SI 2. Chromatograms were integrated
178 using the Cobra detection algorithm from Chromeleon 7.2.8 software. The external
179 calibrations were achieved between 25 ng and 1.4 µg with 6 calibration points (Table 2 and
180 SI 3). The range of the calibration depends greatly on the polymer because the intensity of
181 the indicator compound could vary greatly. The confirmation/quantification ratios were
182 established with the external standards. For the external calibration preparation the
183 polymers were first cryo-milled using the SPEX® SamplePrep 6775 Freezer/Mill cryogenic
184 Grinder (Delta Labo, France) with the program: precool 2 min ; run 1 min ; cool 2 min ;
185 cycles 15 ; cps 15. This inert matrix was prepared from glass microfiber filters (GF/D
186 diameter 47 mm from Whatman®) cryo-milled (precool 1 min; run 1 min; cool 1 min;
187 cycles 6; cps 15) and calcined.

188

189 **2.4 Method Validation and Performance**

190 For each polymer analyzed, an indicator compound was selected for quantification. The
191 analytical limit of detection (LOD) and limit of quantification (LOQ) were determined for
192 each polymer and were defined as S/N of 3 and of 10 respectively. This limit was only
193 reached within the calibration range for PE (130 ng). We selected the following criteria to
194 assess the possibility of determining a peak concentration: 1) the retention time was within
195 a window of 0.05 min compared to that of the standards, 2) the peak was above the
196 analytical LOQ, and 3) there was 30% tolerance in the ratio of the ion transitions. The
197 interday variability will not be discussed as the external calibration standards and the samples
198 were all analyzed in the same sequence on the same day. Finally, a polymer was quantified
199 only if the signal was ten times superior to the procedural and field sampling blanks (Table
200 SI 4) and we did not subtract the signal of the blank to the determined concentration. If any
201 of the above cited criteria were not respected, it was specified that the concentration was
202 not determined (n. d.). The extraction efficiency of the sample preparation was estimated
203 with a positive control that consisted of the 6 polymers in concentrations ranging from 940
204 to 4800 ng/ml of KOH and proceeded with the same steps as those of the preparation and
205 analysis (Table SI 5). To evaluate matrix interferences during pyrolysis or mass
206 spectrometry detection, we proceeded to perform the standard addition method after cryo-

207 grinding was performed for the filters, and the samples were spiked at concentrations of 50
208 to 300 $\mu\text{g/g}$ depending on the polymers.

209 **2.5. Quality Assurance and Quality Control (QA and QC)**

210 A need for stricter QA and QC during method development for microplastic analysis in
211 biota was discussed earlier, and we integrated the criteria proposed in the present study
212 (Hermsen et al., 2018). We took special care to minimize contamination during sampling
213 and during sample preparation in the laboratory. Only glass and metal were used. The only
214 plastic that was in contact with the sample was the opercula in the cap PTFE for sample
215 storage, and this opercula is a polymer that does not interfere with the mass detection of
216 the polymer targeted here. Glass and inox materials were cleaned thoroughly three times
217 with Milli-Q water and ethanol and then systematically calcined prior to use. Laboratory
218 coats that were made of 100% cotton were always worn during the analysis procedures.
219 The work was performed in a fume hood to minimize contamination by airborne
220 microplastics. Whenever the samples were not processed, they were stored in closed glass
221 units. The glass fiber filters were also calcined and stored in glass petri dishes that were
222 wrapped in aluminum foil before use. The quartz tubes that were used for access into the
223 pyrolysis chamber were cleaned at 1000 °C for 30 s immediately before being used and
224 were not stored. The samples in the quartz tube were weighed to minimize airborne
225 contamination, as the tubes were placed in a metal sample holder that was stored in a glass
226 unit with a glass cover. All solvents (water, ethanol, or potassium hydroxide solution) were
227 prefiltered on PTFE (0.45 μm , Omnipore™, from Sigma–Aldrich, St. Louis, MO, USA).
228 The glass microfiber filters were prepared via an optimized calcination (from room
229 temperature to 500 °C at a rate of 80°C/hour with hold of 30 hours at 500°C using a LV
230 5/11 furnace from Nabertherm®).

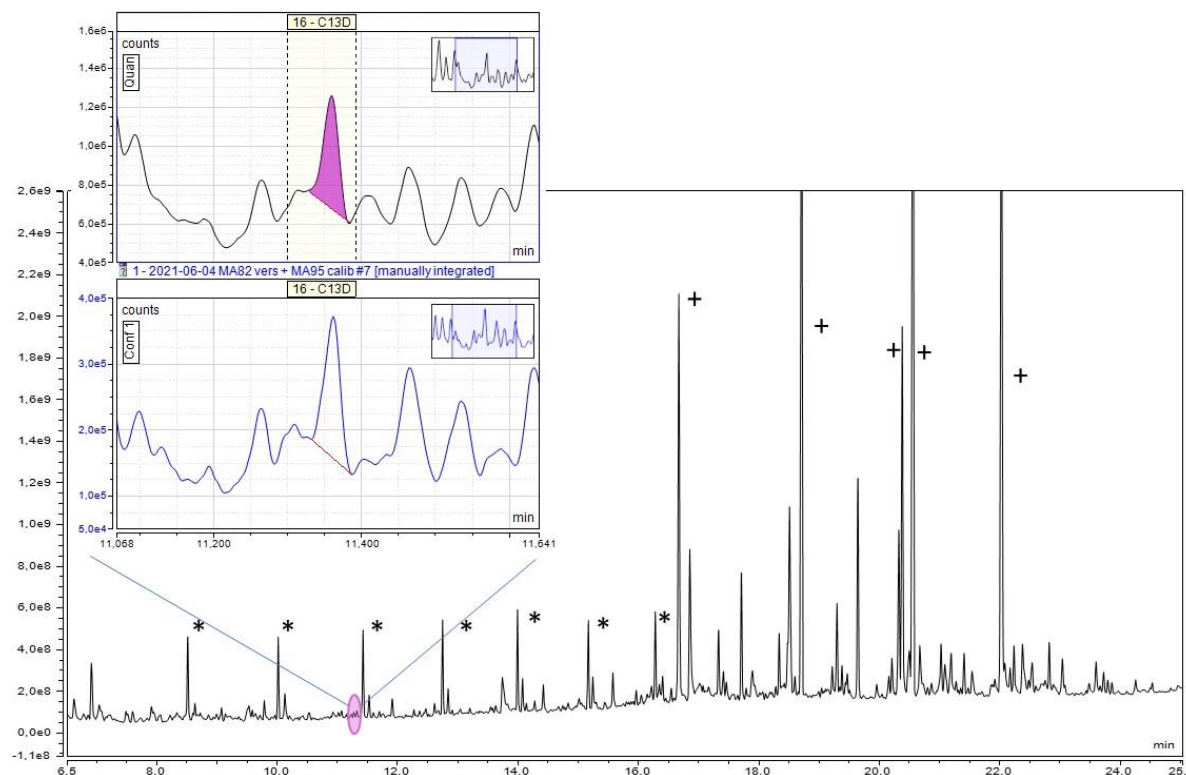
231 **3. Results and Discussion**

232 **3.1. Indicator compound detection and quantification**

233 The method proposed for the identification and quantification of the six targeted polymers
234 (PMMA, PP, PE, PET, PS and PC) is new as it is the first development of tandem mass
235 spectrometry coupled to pyrolysis. The high selectivity of the triple quadrupole allows to
236 shorten the number of steps of the sampling preparation compared to what was proposed
237 with a simple quadrupole (Ribeiro et al., 2020). Because PVC products of pyrolysis are
238 aromatic molecules (like benzene, naphthalene ...) and because they are not specific (there
239 are interferences from organic matter): we excluded this polymer from the study. For PS,

240 we selected the PS trimer as an indicator compound, as in most recent studies (Yakovenko
241 et al., 2020). Styrene cannot be used because it is often a product of natural organic matter
242 pyrolysis (Dierkes et al., 2019; (Fischer and Scholz-Bottcher, 2017; (Zhou et al., 2019).
243 The specific detection of PE has already been discussed considerably because biogenic
244 materials such as natural fats (e.g., fish protein) and waxes are rich in long alkyl chains.
245 They produce n-alkanes and n-alkenes during pyrolysis (Dierkes et al., 2019; (Fischer and
246 Scholz-Bottcher, 2017; (Scholz-Bottcher et al., 2013), which are common products in the
247 pyrolytic decomposition of PE. The selection of an indicator compound among these two
248 families was excluded if there was no intensive sample purification (Okoffo et al., 2020;
249 (Ribeiro et al., 2020). Thus, we opted to use an indicator compound among the n-
250 alkadienes, which are very specific to PE pyrolysis but formed to a much lesser extent
251 (Yakovenko et al., 2020). In this study we selected the congener with 13 carbon atoms
252 (Table 2). In the samples analyzed, we systematically detected PE in the MS/MS mode.
253 The presence of PE was effective because all 3 congeners (the succession of n-alkadienes,
254 n-alkene and n-alkane) were present with an n between 8 and 17. As a demonstration, we
255 reported the signal in the full scan of one sample (Figure 1). The pyrochromatogram is very
256 complex, but the characteristic shape of PE appears in the full scan with the n-alkenes
257 signal (marked with a star in Figure 1). Some fatty acid esters were also present in important
258 proportions and originated from residual organic tissues after chemical digestion. In the
259 inset of Figure 1, the detection of the indicator compound, the n-alkadiene with 13 carbon
260 atoms, is possible with the use of MS/MS. In this insert, we can see that in addition to the
261 indicator compound, we detected many other peaks in MS/MS. Many peaks can be detected
262 in MS/MS (MRM mode) because they have the same transitions as the ones monitored for
263 the C13 target compound which is rather common among hydrocarbon derivatives but the
264 transition ratios are distinct even for structural isomers. All those peaks are hydrocarbons
265 with various unsaturated components and ramifications and are always formed during PE
266 pyrolysis (Sojak et al., 2007). The interference of PE pyrolysis from organic matter,
267 especially with regards of lipids, is a very complex problem which was recently
268 investigated in details (Rauert et al., 2022). In the present study we have considered the
269 ratio C13/C14 as a validation criterion with a tolerance of 30% compared to the ratios
270 recorded for the external standards. Work is under progress to further understand PE
271 pyrolysis and interferences with the matrix investigating several indicator compounds (the
272 ratios recorded for the samples are presented in figure SI 1). In a recent review paper, we

273 argued for the choice of indicator compound selections for the other polymers (Yakovenko
274 et al., 2020).



275
276

277 Figure 1: Full scan analysis of the *Amphiura filiformis* sample. The stars mark the peaks of
278 the n-alkene congeners; they are the main products of pyrolytic PE decomposition. The
279 peaks marked with a cross are fatty acid esters and remains of the tissues of the animals
280 after chemical digestion. In the inset box, the signal of the selected indicator compound of
281 PE is presented in the MS/MS; we chose the alkadiene congener with 13 carbon atoms
282 because its signal was the highest.

283 3.2 Sample digestion efficiency and evaluation of polymer integrity

284 We selected a chemical digestion protocol using potassium hydroxide to remove the
285 organic tissues. The efficiency of this protocol was discussed considerably, and potassium
286 hydroxide appeared to be a good compromise for obtaining an efficient purification and
287 preserving the polymers (Dehaut et al., 2016). We observed that even if the organisms
288 sampled were very distinct in terms of their taxonomic species, size, weight and feeding
289 modes, the protocol was well adapted to this diversity. The digestion efficiency was
290 estimated by mass balance; we determined that between 97 and 80% of the samples weight
291 was eliminated. The elementary analysis of the remaining matter showed less than 0.3 %
292 of organic carbon; we are assuming that the material left after chemical digestion was

293 mainly inorganic. This is in accordance with the fact that some organisms were deposit
294 feeders and that they are ingesting sediment particles. The samples with the lowest
295 digestion efficiencies corresponded to *Glandiceps talaboti* and *Notomastus* sp., which are
296 subsurface deposit feeders. Such organisms typically process at least one body weight of
297 sediment daily. As a consequence, their alimentary tract contains large volumes of
298 sediment that are not eliminated during chemical digestion (Lopez and Levinton, 1987).
299 These results underlined the importance of the weight-specific feeding rates to be
300 considered when characterizing the plastic that is ingested by benthic species.

301 Compared to enzymatic digestion, chemical digestion offers many advantages since it is
302 very efficient and not expensive, but a disadvantage is the possible alteration of some
303 polymers. It was recently reported that even if PET was resistant to digestion when
304 potassium hydroxide was used at 60 °C, smaller particles, such as PET fibers, did not resist
305 such temperatures; thus, lower temperatures are recommended (Treilles et al., 2020). For
306 instance, the digestion of seafood samples at 60 °C resulted in 32% recoveries for PET
307 (Ribeiro and al. 2020). For this reason, chemical digestion was performed at 40 °C. We
308 obtained an extraction procedure efficiency for the six spiked polymers between 82 and
309 129%, which was within the precision margin of the MS/MS method, so we estimated that
310 the recoveries were acceptable (Table SI 5).

311 **3.3. Method Validation and Performance**

312 To proceed to the fabrication of the external calibration we first cryo-milled the polymer
313 separately. They were then mixed in an inert glass fiber matrix also previously grinded
314 and calcined to remove any trace of polymers. The external standards were first prepared
315 at concentrations ranging from 1 mg.g⁻¹ to 5 mg.g⁻¹ and the powder was then diluted by a
316 factor 10. To obtain the external calibration we prepared 5 dilutions to reach the calibration
317 range detailed Table SI 3. The repeated injection of an external standard (N=12) showed a
318 standard deviation below 20% for all polymers considered. We thus consider the
319 homogenization of the powders was satisfactory. The response was linear within the
320 calibration range for each polymer with a correlation value (R²) greater than 0.85 (Table
321 2). After digestion and filtration of the samples on glass fiber filters, the filters were cryo-
322 ground to present good homogeneity, as only a fraction, typically 2 mg, was introduced in
323 the pyrolysis chamber. After cryo-grinding, a sample analyzed in triplicate showed a
324 standard deviation below 35% for all polymers considered (Table SI 6). We estimated that

325 cryo-grinding was efficient and that the sample was sufficiently homogeneous. The other
326 samples were analyzed once.

327 The procedural and field blank polymer concentrations are presented in Table SI 4. The
328 amount of PMMA in the samples was not determined because the concentrations in the
329 sampling control blank were rather important (4.7 $\mu\text{g/g}$ filter, table SI 4). Further studies
330 are needed to determine the potential source of contamination and to improve the QA/QC
331 for this polymer.

332 The potential impact of the remaining matter after chemical digestion on the polymer
333 analysis was assessed with the standard addition method. The pyrolytic fingerprint of all
334 the polymers was identical when the polymers were injected as a pure sample or within the
335 matrix, indicating that the presence or residual organic or inorganic matter did not interfere
336 with the polymer pyrolysis or the MS/MS detection. The case of PE is remarkable because
337 some natural organic molecules (like lipids) could thermally decompose into dienes as it
338 was recently reported (Rauert et al., 2022). In order to ensure that the remaining matter
339 after sample preparation did not enhance the signal of PE we used an additional validation
340 criterion based on the recording of two indicator compounds (the analogues with 13 and
341 14 carbon atoms). The ratios recorded and compared to the external standards are reported
342 in Figure SI 1.

343 Table 2: Polymers targeted together with the indicator compound selection and external
344 calibration characteristics.

Polymer	Indicator compound	Quantification transition (m/z)	External calibration range (μg)	Numbers of point	r^2
<i>PMMA</i>	methyl methacrylate	100>41	35 to 380 ng	6	0.98
<i>PP</i>	2,4-dimethylhept-1-ene	70>55	30 to 300 ng	5	0.90
<i>PE</i>	1,12-tridecadiene	95>67	130 to 1360 ng	6	0.88
<i>PET</i>	dimethyl terephthalate	163>135	25 to 265 ng	6	0.96
<i>PS</i>	5-hexene-1,3,5-triyltribenzene (styrenetrimer)	207>129	50 to 385 ng	5	0.99

<i>PC</i>	2,2-bis(4'-methoxy-phenyl)propane	241>133	27 to 280 ng	6	0.95
-----------	-----------------------------------	---------	--------------	---	------

345

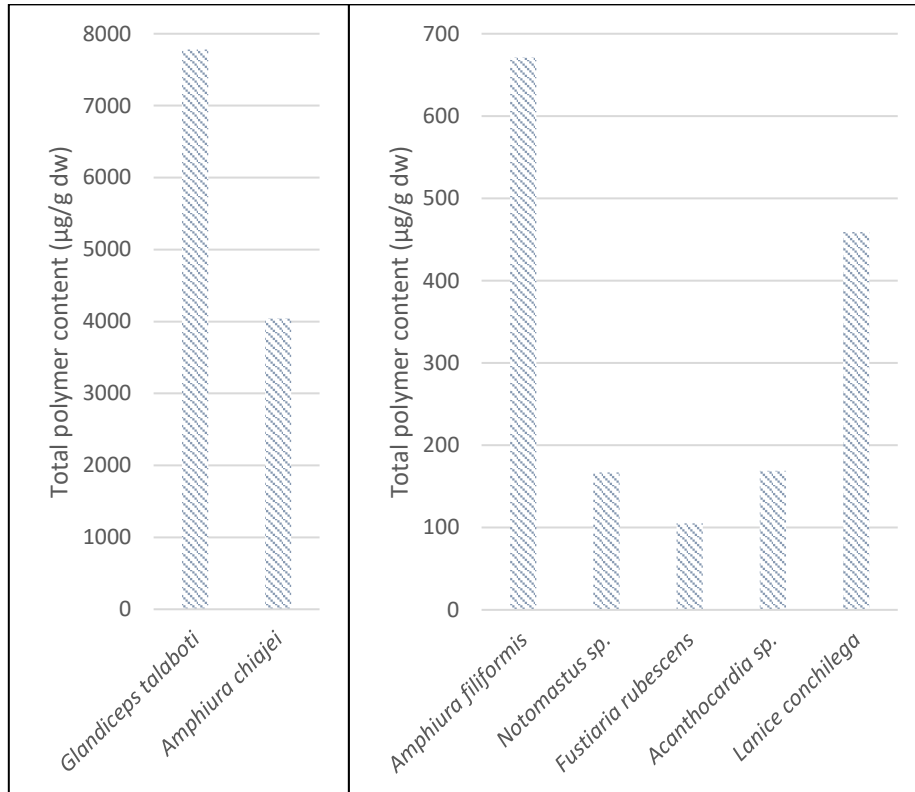
346 **3.4. Polymer content in the samples**

347 In general, we systematically detected plastic in the marine benthic animals analyzed. The
 348 total polymer contents (Figure 2 and Table SI 7) varied from one specimen to another and
 349 were between 105 and 7780 µg/g dry weight. These margins are within those recently
 350 determined by Py-GC–MS for seafood (Ribeiro et al., 2020). There is not yet an established
 351 pattern between the content of plastic in marine organisms and the feeding modes, marine
 352 habitat or trophic position, even with a large sample set. Microplastic accumulation in the
 353 marine food chain has been supported by some authors (Carbery et al., 2018), while a recent
 354 critical review concluded that no plastic biomagnification occurred (Walkinshaw et al.,
 355 2020). The authors argued that microplastics do not translocate from the digestive system
 356 into tissues or into circulatory fluid and that microplastics are only transitory contaminants
 357 with a limited residence time within organisms. Nevertheless, the mechanisms of plastic
 358 particle ingestion, egestion or excretion are still not well understood (Cole et al., 2016). In
 359 general, authors assume that the residence time of plastic particle in the digestive system
 360 is deeply correlated with the particle size, shape and rugosity, which are very
 361 heterogeneous in the environment and could explain the great variations obtained between
 362 specimens, in addition to ecological or environmental factors.

363 In our study, we collected species with variable feeding modes. *Glandiceps talaboti*,
 364 *Notomastus* sp. and *Amphiura chiajei* are strict deposit feeders (Buchanan, 1964), while
 365 *Lanice conchilega* is both a suspension feeder and deposit feeder, depending on the
 366 environmental conditions (Word, 1990; (Zarkanellas and Kattoulas, 1982). *Amphiura*
 367 *filiformis* is known to have a main filtering activity (Buchanan, 1964). *Acanthocardia*
 368 *paucicostata* is a strict suspension feeder, and *Fustiaria rubescens* is a carnivorous feeding
 369 mainly on foraminifers from sediment surfaces (Gofas et al., 2011). These species are
 370 known to be good integrators of environmental variation because of their reduced mobility.
 371 Therefore, their plastic content may be considered a good proxy of the plastic content of
 372 the environment in the same region, with the limit of the spatial heterogeneity of
 373 microplastics on the sea floor. Overall, our results agreed with this hypothesis by indicating
 374 that the type of polymer recovered from benthic animals with different feeding modes
 375 corresponds to the distribution of the polymer in the oceans. Nonetheless we observed

376 important variation among individuals; this variability was often reported and is not yet
377 explained (Ribeiro et al., 2020).

378
379



380
381
382
383

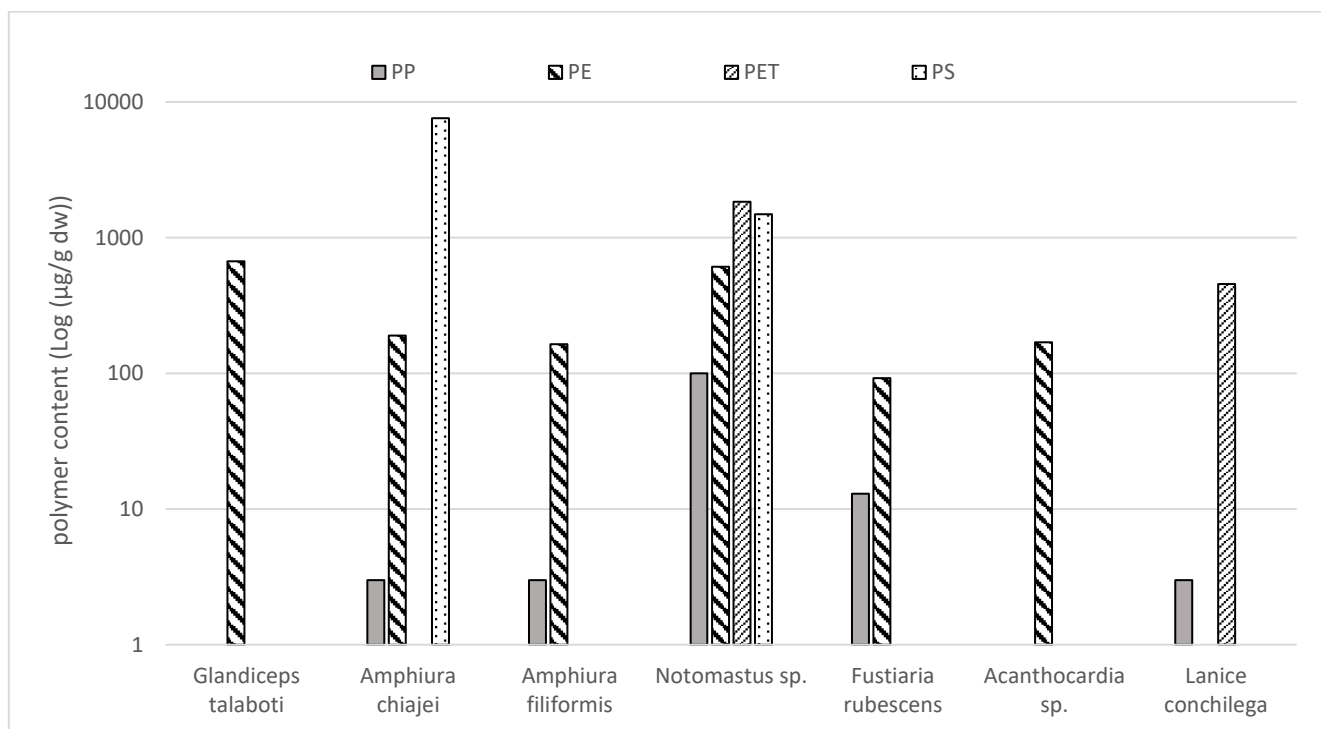
Figure 2: Total polymer content expressed in µg per gram of dry weight (µg/g dw).

384 PE was detected in six samples of the seven analyzed samples (Figure 3) at concentrations
385 up to 670 µg/g dw for the *Glandiceps talaboti* individual. We noticed that PE was often
386 present in the largest proportions, often superior to 80% of the total polymer content. It has
387 been reported that PE was dominant in marine samples with an average proportion of 42%
388 at the sea surface and with a decrease in abundance through the water column (Erni-Cassola
389 et al., 2019). Our results agreed with those of Missawi et al., who reported that PE was
390 dominant in the polychaete worm *Hediste diversicolor* on the Tunisian coast in the
391 Mediterranean Sea, with important variations among individuals and sites, whereas PP was
392 detected in lesser proportions than those of PE (Missawi et al., 2020), which is in
393 accordance with the reported concentrations at sea (Erni-Cassola et al., 2019).

394 *Notomastus sp.* et *Lanice conchilega* presented high contents of PET, which are likely to
395 be associated with deposit feeders because it is a polymer with a higher density than that
396 of sea water. Previous studies using spectroscopic characterization emphasized that a high

397 proportion of PETs were detected in detritivores, which corresponds to plastic fibers (Renzi
 398 et al., 2020). PET fibers have also been detected in high proportions in seafloor samples
 399 (Kane et al., 2020). Figure 3 also shows that *Amphiura chiajei* and *Notomastus sp.*
 400 exhibited a high content of PS. They are both deposit feeders and are likely exposed to
 401 denser polymers such as PS. Along the same line, PMMA, which is also known to be more
 402 abundant in the sediment than at its surface (Renzi et al., 2020), has not been detected in
 403 suspension feeders such as *A. filiformis* and *A. paucicostata*. This could be explained by
 404 the relatively high limit of detection for PMMA under our conditions.

405



406

407 Figure 3: Polymer content in the benthic individuals (expressed in µg/g dry weight).
 408

409 **Concluding remarks**

410 The study demonstrates that a method based on Py-GC-MS/MS leads to a simplified
 411 sample purification and enables microplastic contents down to 0.7 µm to be determined
 412 with good reliability in organisms. Py-GC-MS does not provide information on the color,
 413 shape, or size of microplastics and is complementary to methods that are based on
 414 spectroscopy (Primpke et al., 2020). The use of pyrolysis to quantify microplastics still
 415 involves limitations and areas of improvement that need to be considered before it becomes
 416 a standardized technique. As a first glance, the use of internal standards will certainly

417 improve the precision of the measurements even if the developments in this direction
418 present some technical difficulties (Lauschke et al., 2021) that are challenging because very
419 few isotopic analog resins are commercially available. Other important undertakings
420 involve achieving a better understanding of matrix interference and the effect of polymer
421 weathering on the pyrolytic response (Ainali et al., 2021; (Biale et al., 2021; (Toapanta et
422 al., 2021). The most appealing aspect of Py-GC–MS is that it does not have size limitations,
423 as there is still very little known about the behavior of small microplastics in the
424 environment and their interaction with organisms. We emphasize the promising potential
425 for the use of Py-GC–MS as it involves straightforward sample preparation, even with
426 complex samples, and the possibility of increasing our capacity to analyze larger sample
427 sets for environmental assessments. To gain a better understanding of the interactions of
428 benthic community with plastic pollution, the variation in plastic concentrations with
429 sediment depth at different locations should be investigated, and this could be first explored
430 by focusing on a single species with a strict feeding mode.

431

432

Supporting material

433

434

435 **Determination of the microplastic content in Mediterranean benthic**
436 **organisms by pyrolysis-gas chromatography-tandem mass**
437 **spectrometry**

438 Magali Albignac¹, Jean François Ghiglione², Céline Labrune³, Alexandra ter Halle^{1*}

439 ¹CNRS, Université de Toulouse, Laboratoire des Interactions Moléculaires et Réactivité Chimique
440 et Photochimique (IMRCP), UMR 5623, Toulouse, France

441 ²CNRS, Sorbonne Université, Laboratoire d'Océanographie Microbienne (LOMIC), UMR 7621,
442 Observatoire Océanologique de Banyuls, Banyuls sur mer, France

443 ³CNRS, Sorbonne Université, Laboratoire d'Ecogéochimie des Environnements Benthiques
444 (LECOB), UMR 8222, Observatoire Océanologique de Banyuls, Banyuls sur mer, France

445

446 **Table SI1:** Optimized conditions for Pyrolysis-GCMS/MS

447

Pyrolyzer

Carrier gas helium

Pyrolysis temperature 600°C

Pyrolysis time 30 s

Gas chromatogram

Initial temperature 40°C

Flow 1.25 mL.min⁻¹

Temperature program 40°C (2 min) => 300°C (5 min) at 10°C.min⁻¹

Transfer line temperature 280°C

Mass spectrometer

Mode Multiple Reaction Monitoring

Scan time 0.15 s

Source temperature 300°C

448

449 Table SI 2: Additional information for polymer detection and quantification after MS/MS
 450 development.
 451

Indicator compound	Retention time	Quantification transition (Tq)	Confirmation transition (Tc)	Tc/Tq (%)*
<i>Methyl-methacrylate</i>	2.73	100>41 (15eV)	100>69 (10eV)	76.1
<i>Dimethyle-heptene</i>	4.47	70>55 (10 eV)	126>83 (5 eV)	13.9
<i>1,12 tridecadiene</i>	11.36	95>67 (10 eV)	109>67 (10 eV)	43.1
<i>Dimethylterephthalate</i>	14.33	163>135 (10 eV)	163>103 (15 eV)	69.9
<i>StyreneTrimere</i>	23.4	207>129 (10 eV)	207>91 (15 eV)	46.7
<i>Methyl-bis-phenol A</i>	20.26	241>133 (15 eV)	256>241 (10 eV)	81.3

452
 453 *The ratio Tc/Tq was determined over the first 3 most concentrated external standards
 454 injected for the calibration
 455 ** Typically, we introduce 2 mg of standard or sample for pyrolysis analysis
 456

457 **Table SI 3:** External standards amount injected range and MS/MS peak intensity.

Polymer	Range of concentration of the 6 calibration points (ng)	Range of corresponding peak area for the transition of quantification
PMMA	37 - 384	1E+05 - 2E+06
PP	30 - 309	1E+05 - 8E+05
PE	133 - 1357	8E+03 - 9E+04
PET	26 - 264	6E+04 - 3E+06
PC	50 - 508	7E+04 - 1E+06
PS	27 - 280	1E+06 - 2E+07

458

459 Table SI 4: Amount of polymer detected in the sampling control and the procedural control.

Polymer targeted	Sampling control blank	Procedural control
<i>PMMA</i> ($\mu\text{g/g}$)	4.7	2.7
<i>PP</i> ($\mu\text{g/g}$)	n.d	n.d.
<i>PE</i> ($\mu\text{g/g}$)	n.d	n.d.
<i>PET</i> ($\mu\text{g/g}$)	40.0	0.8
<i>PS</i> ($\mu\text{g/g}$)	4.0	0.7
<i>PC</i> ($\mu\text{g/g}$)	n.d	n.d.

460
461
462
463
464

n.d.: not determined. The indicator compound peak was not detected, and the Tq/Tc ratio was not confirmed.

465 Table SI 5: Digestion recoveries for the polymers with the standard addition method

Polymer targeted	Concentrations of the polymer in the inert matrix ($\mu\text{g}\cdot\text{g}^{-1}$)	Amount of polymer added for the recovery test (ng)	Proportion of polymer recovered after chemical digestion (%)
<i>PMMA</i>	607	6182	107
<i>PP</i>	489	4978	82
<i>PE</i>	2147	4260	111
<i>PET</i>	418	4513	129
<i>PS</i>	804	8196	122
<i>PC</i>	443	9036	116

466

467

468 Table SI 6: The *Lanice conchilega* sample was analyzed in triplicate. The relative
469 standard deviations were reported for all polymers and did not exceed 35%.

470

Polymer targeted	Indicator compound	SD - %
<i>PMMA</i>	Methyl-methacrylate	19
<i>PP</i>	Dimethyle-heptene	23
<i>PE</i>	1,12 tridecadiene	24
<i>PET</i>	Dimethylterephthalate	29
<i>PS</i>	StyreneTrimere	34
<i>PC</i>	Methyl-bis-phenol A	10

471

472

473 Table SI 7: Concentration of the polymer targeted expressed in μg per gram of dry wet
 474 ($\mu\text{g/g}$ dw). The results are presented with a standard deviation of 35%.

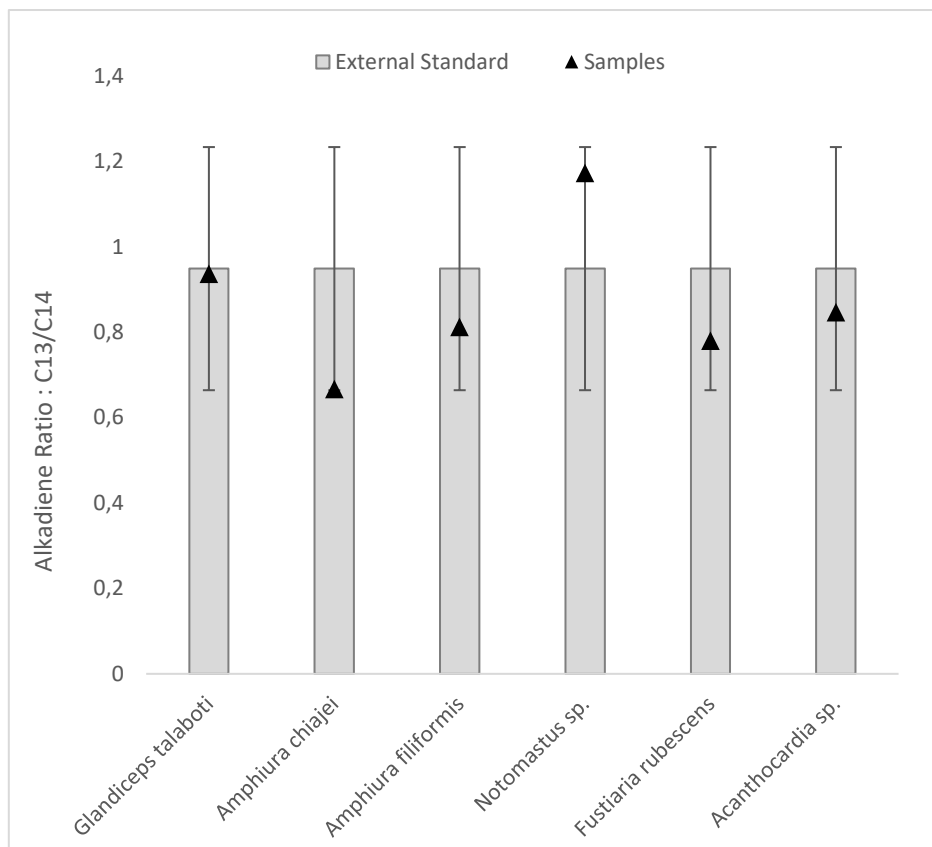
475

Sample N°	2	3	4	5	6	7	8
	Glandiceps talaboti	Amphiura chiajei	Amphiura filiformis	Notomastus sp.	Fustiaria rubescens	Acanthocardia sp.	Lanice conchilega
<i>PMMA</i> ($\mu\text{g/g}$)	n.d.	n.d.	n.d.	n.d.	n.d.	n.d.	n.d.
<i>PP</i> ($\mu\text{g/g}$)	1	3	3	100	13	n.d.	3
<i>PE</i> ($\mu\text{g/g}$)	670	190	164	610	92	169	n.d.
<i>PET</i> ($\mu\text{g/g}$)	n.d.	n.d.	n.d.	1845	n.d.	n.d.	456
<i>PS</i> ($\mu\text{g/g}$)	n.d.	7587	n.d.	1487	n.d.	n.d.	n.d.
<i>PC</i> ($\mu\text{g/g}$)	n.d.	n.d.	n.d.	23	n.d.	n.d.	n.d.

476

477 n.d.: the concentrations were not determined.

478



479

480 Figure SI 1 : Ratio of the peak areas for the two indicator compounds selected to monitor
 481 PE: the alkadienes congeners with 13 and 14 carbons atoms. The grey bars represent the
 482 mean values calculated for the external standards (within the calibration range presented)
 483 and the black triangles represent the values obtained for the samples. The error bars set at
 484 30% represent the validation criterion adopted to ensure that PE quantification exclude
 485 the signal of natural organic matter.

486

487
488
489
490
491
492
493
494
495
496
497
498
499
500
501
502
503
504
505
506
507
508
509
510
511
512
513
514
515
516
517
518
519
520
521
522
523
524
525
526
527
528
529
530
531
532
533
534
535
536
537
538

References

- Ainali, N.M., et al., 2021. Aging effects on low- and high-density polyethylene, polypropylene and polystyrene under UV irradiation: An insight into decomposition mechanism by Py-GC/MS for microplastic analysis. *Journal of Analytical and Applied Pyrolysis* 158. <https://doi.org/10.1016/j.jaap.2021.105207>.
- Anastasopoulou, A., et al., 2013. Plastic debris ingested by deep-water fish of the Ionian Sea (Eastern Mediterranean). *Deep-Sea Research Part I-Oceanographic Research Papers* 74, 11-13. <https://doi.org/10.1016/j.dsr.2012.12.008>.
- Angiolillo, M., et al., 2021. Distribution of seafloor litter and its interaction with benthic organisms in deep waters of the Ligurian Sea (Northwestern Mediterranean). *Sci. Total Environ.* 788. <https://doi.org/10.1016/j.scitotenv.2021.147745>.
- Biale, G., et al., 2021. A Systematic Study on the Degradation Products Generated from Artificially Aged Microplastics. *Polymers* 13. <https://doi.org/10.3390/polym13121997>.
- Buchanan, J.B., 1964. A comparative study of some features of the biology of *Amphiura filiformis* and *Amphiura chiajei* (Ophiuroidea) considered in relation to their distribution. *J Mar Biol Ass UK* 44, 615-624.
- Carbery, M., et al., 2018. Trophic transfer of microplastics and mixed contaminants in the marine food web and implications for human health. *Environ Int* 115, 400-409. <https://doi.org/10.1016/j.envint.2018.03.007>.
- Cole, M., et al., 2016. Microplastics Alter the Properties and Sinking Rates of Zooplankton Faecal Pellets. *Environ. Sci. Technol.* 50, 3239-3246. <https://doi.org/10.1021/acs.est.5b05905>.
- Coll, M., et al., 2010. The Biodiversity of the Mediterranean Sea: Estimates, Patterns, and Threats. *Plos One* 5. <https://doi.org/10.1371/journal.pone.0011842>.
- Consli, P., et al., 2020. Characterization of seafloor litter on Mediterranean shallow coastal waters: Evidence from Dive Against Debris (R), a citizen science monitoring approach. *Marine Pollution Bulletin* 150. <https://doi.org/10.1016/j.marpolbul.2019.110763>.
- Danovaro, R., et al., 2020. Towards a marine strategy for the deep Mediterranean Sea: Analysis of current ecological status. *Marine Policy* 112. <https://doi.org/10.1016/j.marpol.2019.103781>.
- de Madron, X.D., et al., 2017. Deep sediment resuspension and thick nepheloid layer generation by open-ocean convection. *J Geophys Res-Oceans* 122, 2291-2318. <https://doi.org/10.1002/2016jc012062>.
- Dehaut, A., et al., 2016. Microplastics in seafood: Benchmark protocol for their extraction and characterization. *Environ. Pollut.* 215, 223-233. <https://doi.org/10.1016/j.envpol.2016.05.018>.
- Dierkes, G., et al., 2019. Quantification of microplastics in environmental samples via pressurized liquid extraction and pyrolysis-gas chromatography. *Anal Bioanal Chem* 411, 6959-6968. <https://doi.org/10.1007/s00216-019-02066-9>.
- Erni-Cassola, G., et al., 2019. Distribution of plastic polymer types in the marine environment; A meta-analysis. *J. Hazard. Mater.* 369, 691-698. <https://doi.org/10.1016/j.jhazmat.2019.02.067>.
- Fischer, M., Scholz-Bottcher, B.M., 2017. Simultaneous Trace Identification and Quantification of Common Types of Microplastics in Environmental Samples by Pyrolysis-Gas Chromatography-Mass Spectrometry. *Environ. Sci. Technol.* 51, 5052-5060. <https://doi.org/10.1021/acs.est.6b06362>.
- Galgani, F., et al., 2000. Litter on the sea floor along European coasts. *Marine Pollution Bulletin* 40, 516-527. [https://doi.org/10.1016/s0025-326x\(99\)00234-9](https://doi.org/10.1016/s0025-326x(99)00234-9).
- Galgani, F., et al., 1996. Accumulation of debris on the deep sea floor off the French Mediterranean coast. *Mar Ecol Prog Ser* 142, 225-234. <https://doi.org/10.3354/meps142225>.
- Galloway, T.S., et al., 2017. Interactions of microplastic debris throughout the marine ecosystem. *Nat Ecol Evol* 1. <https://doi.org/10.1038/s41559-017-0116>.
- Ghiglione, J.F., Laudet, V., 2020. Marine Life Cycle: A Polluted Terra Incognita Is Unveiled. *Current Biology* 30, R130-R133. <https://doi.org/10.1016/j.cub.2019.11.083>.
- Gofas, S., et al. (2011) *Moluscos marinos de Andalucia*.

539 Hall, S.J., 2002. The continental shelf benthic ecosystem: current status, agents for change and
540 future prospects. *Environmental Conservation* 29, 350-374.
541 <https://doi.org/10.1017/s0376892902000243>.

542 Hermsen, E., et al., 2018. Quality Criteria for the Analysis of Microplastic in Biota Samples: A
543 Critical Review. *Environ. Sci. Technol.* 52, 10230-10240. <https://doi.org/10.1021/acs.est.8b01611>.

544 Kane, I.A., et al., 2020. Seafloor microplastic hotspots controlled by deep-sea circulation. *Science*
545 368, 1140-+. <https://doi.org/10.1126/science.aba5899>.

546 Kooi, M., et al., 2017. Ups and Downs in the Ocean: Effects of Biofouling on Vertical Transport of
547 Microplastics. *Environ. Sci. Technol.* 51, 7963-7971. <https://doi.org/10.1021/acs.est.6b04702>.

548 Lauschke, T., et al., 2021. Evaluation of poly(styrene-d5) and poly(4-fluorostyrene) as internal
549 standards for microplastics quantification by thermoanalytical methods. *Journal of Analytical and*
550 *Applied Pyrolysis* 159. <https://doi.org/10.1016/j.jaap.2021.105310>.

551 Lopez, G.R., Levinton, J.S., 1987. Ecology of deposit-feeding animals in marine-sediments.
552 *Quarterly Review of Biology* 62, 235-260. <https://doi.org/10.1086/415511>.

553 Manea, E., et al., 2020. Towards an Ecosystem-Based Marine Spatial Planning in the deep
554 Mediterranean Sea. *Sci. Total Environ.* 715. <https://doi.org/10.1016/j.scitotenv.2020.136884>.

555 Missawi, O., et al., 2020. Abundance and distribution of small microplastics ($\leq 3 \mu m$) in
556 sediments and seaworms from the Southern Mediterranean coasts and characterisation of their
557 potential harmful effects. *Environ. Pollut.* 263. <https://doi.org/10.1016/j.envpol.2020.114634>.

558 Okoffo, E.D., et al., 2020. Identification and quantification of selected plastics in biosolids by
559 pressurized liquid extraction combined with double-shot pyrolysis gas chromatography-mass
560 spectrometry. *Sci. Total Environ.* 715. <https://doi.org/ARTN> 136924
561 10.1016/j.scitotenv.2020.136924.

562 Pico, Y., Barcelo, D., 2020. Pyrolysis gas chromatography-mass spectrometry in environmental
563 analysis: Focus on organic matter and microplastics. *Trac-Trend Anal Chem* 130.
564 <https://doi.org/ARTN> 115964 10.1016/j.trac.2020.115964.

565 Primpke, S., et al., 2020. Comparison of pyrolysis gas chromatography/mass spectrometry and
566 hyperspectral FTIR imaging spectroscopy for the analysis of microplastics. *Anal Bioanal Chem* 412,
567 8283-8298. <https://doi.org/10.1007/s00216-020-02979-w>.

568 Rauert, C., et al., 2022. Extraction and Pyrolysis-GC-MS analysis of polyethylene in samples with
569 medium to high lipid content. *Journal of Environmental Exposure Assessment* 1, 13.
570 <https://doi.org/10.20517/jeea.2022.04>.

571 Renzi, M., et al., 2020. Chemical composition of microplastic in sediments and protected
572 detritivores from different marine habitats (Salina Island). *Marine Pollution Bulletin* 152.
573 <https://doi.org/10.1016/j.marpolbul.2020.110918>.

574 Ribeiro, F., et al., 2020. Quantitative Analysis of Selected Plastics in High-Commercial-Value
575 Australian Seafood by Pyrolysis Gas Chromatography Mass Spectrometry (vol 54, pg 9408, 2020).
576 *Environ. Sci. Technol.* 54, 13364-13364. <https://doi.org/10.1021/acs.est.0c05885>.

577 Scholz-Bottcher, B.M., et al., 2013. An 18th century medication "Mumia vera aegyptica" - Fake or
578 authentic? *Organic Geochemistry* 65, 1-18. <https://doi.org/10.1016/j.orggeochem.2013.09.011>.

579 Schwaferts, C., et al., 2019. Methods for the analysis of submicrometer- and nanoplastic particles
580 in the environment. *Trends Anal. Chem.* 112, 52-65. <https://doi.org/10.1016/j.trac.2018.12.014>.

581 Sojak, L., et al., 2007. High resolution gas chromatographic-mass spectrometric analysis of
582 polyethylene and polypropylene thermal cracking products. *Journal of Analytical and Applied*
583 *Pyrolysis* 78, 387-399. <https://doi.org/10.1016/j.jaap.2006.09.012>.

584 Toapanta, T., et al., 2021. Influence of surface oxidation on the quantification of polypropylene
585 microplastics by pyrolysis gas chromatography mass spectrometry. *Sci. Total Environ.* 796.
586 <https://doi.org/10.1016/j.scitotenv.2021.148835>.

587 Treilles, R., et al., 2020. Impacts of organic matter digestion protocols on synthetic, artificial and
588 natural raw fibers. *Sci. Total Environ.* 748. <https://doi.org/ARTN> 141230
589 10.1016/j.scitotenv.2020.141230.

590 Tubau, X., et al., 2015. Marine litter on the floor of deep submarine canyons of the Northwestern
591 Mediterranean Sea: The role of hydrodynamic processes. *Prog Oceanogr* 134, 379-403.
592 <https://doi.org/10.1016/j.pocean.2015.03.013>.

593 Valente, T., et al., 2020. Macro-litter ingestion in deep-water habitats: is an underestimation
594 occurring? *Environmental Research* 186. <https://doi.org/10.1016/j.envres.2020.109556>.

595 Walkinshaw, C., et al., 2020. Microplastics and seafood: lower trophic organisms at highest risk of
596 contamination. *Ecotoxicology and Environmental Safety* 190.
597 <https://doi.org/10.1016/j.ecoenv.2019.110066>.

598 Word, J.Q., 1990. The infaunal trophic index, a functional approach to benthic community
599 analyses.

600 Yakovenko, N., et al., 2020. Emerging use thermo-analytical method coupled with mass
601 spectrometry for the quantification of micro(nano)plastics in environmental samples. *TrAC Trends*
602 *in Analytical Chemistry* 131, 115979. <https://doi.org/https://doi.org/10.1016/j.trac.2020.115979>.

603 Zarkanellas, A.J., Kattoulas, M.E., 1982. The Ecology of Benthos in the Gulf of ThermaTkos, Greece.
604 *Marine Ecology* 3, 21-39.

605 Zhou, X.X., et al., 2019. Cloud-Point Extraction Combined with Thermal Degradation for
606 Nanoplastic Analysis Using Pyrolysis Gas Chromatography-Mass Spectrometry. *Analytical*
607 *Chemistry* 91, 1785-1790. <https://doi.org/10.1021/acs.analchem.8b04729>.

608

609